Shape-persistent polyphenylene dendrimers: a computational study

Sabrina Pricl*, Maurizio Fermeglia, Marco Ferrone

Computer-aided Systems Laboratory, Department of Chemical, Environmental and Raw Materials Engineering -DICAMP, University of Trieste, Piazzale Europa 1, 34127 Trieste, Italy

Phil Carrion

European Associates for Environment, via Don Minzoni 17, Gradisca d'Isonzo (Go), Italy

Abstract

3D polyphenylene dendrimers (PDs) can be prepared in ways that enable control of their shape, and their structures may be used as scaffolds with a wide variety of functionality, enabling them to be used as functional nanoparticles with a wide variety of possible applications, ranging from light emitting devices to biological sensors or drug delivery tools. As PDs have been synthesized only recently, their structural and chemico-physical characterization is still in its infancy. Accordingly, in this paper the shape and internal organization of two PD families based on two different cores were probed by accurate, atomistic molecular dynamics simulations (MD). Particular care was taken to ensure complete structural equilibration by using an ad hoc developed force field and implementing a MD simulated annealing protocol prior to evaluation of the molecular structure and dynamics. Both dendrimer families were found to be characterized by molecular dimensions in the nano-range, and by a shape-persistent, non-spherical structure, of molecular fractal dimension around 2.5-2.6, and of surface fractal dimension practically constant and almost equal to 2 with increasing generations in both cases. The MD analysis revealed also that, for this type of dendrimers, the starburst limited generation is presumably located in correspondence of the third generation.

* Corresponding author e-mail: sabrinap@dicamp.units.it

1. INTRODUCTION

Polymers, with their large spatial extent and chemical variety, afford materials scientists the opportunity to be architects at the molecular level. Once the architecture is decided, however, the task of construction moves to the chemical engineer to build the material in a faithful, stable and efficient manner. This involves assembly not only the molecular structure but also the larger scale internal micro- and meso-structure of the material. New processes are continually becoming available to the chemical engineer to accomplish this end. Innovative catalysts, original macromolecular building blocks, reactive processing, self-assembly, manipulation of phase behavior, applications of strong orienting fields and genetic engineering of materials are just a few examples of the plethora of tools available nowadays to the chemical engineer for the design and production of novel polymeric materials.

End-use properties, which are the ultimate measure of the efficacy of a polymer manufacturing operation, are generally affected as much by the chemical and physical processing as by the molecular design. Polymer production is not simply a matter of executing the molecular blueprint. There is a level of interaction between the process and the product with polymers which is much richer, more complex and more intricate that for most chemical products. Polymer properties are not intrinsic, as are the properties of simple chemicals, but rather they can be manipulated widely by polymerization and processing conditions. For this reason, chemical engineers producing polymers must be conversant in molecular design, and molecular designers must be aware of processing considerations.

An intriguing development in the last decade is the burst of activity in the design, synthesis and applications of dendrimer polymers (Tomalia et al., 1990; Mekelburger et al., 1992; Frechét, 1994; Voit, 1995; Fischer and Vögtle, 1999; Dykes, 2001). The

term *functional polymer* is often used to describe polymers that carry reactive functional groups that can participate in chemical processes without degradation of the original polymeric unit. Functional polymers are abundant in nature. Molecular architecture has significant effects on the characteristics of functional polymers. Most polymers consist of largely linear chains that are randomly coiled and entangled with their neighbors. Introduction of substantial amounts of branching is always accompanied by substantial changes in thermophysical properties, such as viscosity and density. From the point of view of functionalization, a major effect of branching is the multiplication of reactive chain ends.

Dendrimers are highly branched, three-dimensional macromolecules with branch points at every monomer, leading to a structure that has essentially as many end-groups as it has monomeric units. When synthesized by controlled, convergent growth, these dense, regular structures tend to adopt compact, well-defined shapes and, in initial explorations, have begun to exhibit physical properties not seen even in other more traditional forms of highly branched polymers (Tomalia et al., 1990). In this introduction, we can just briefly summarize some of the exciting, new applications for dendrimers actually being explored in industry and university. These include uses as polymeric catalyst particle and nanoscale reactors (Brunner, 1995; Fan et al., 2000), molecular mimics of micelles (Hawker et al., 1993; Pan and Ford, 2000), delivery vehicles for drugs (Esfand and Tomalia, 2001), magnetic resonance imaging agents (Stiriba et al., 2002), immuno-diagnostic and gene therapy (Lynn and Langer, 2000; Ohashi et al., 2001), synthetic mimics of protein active sites (Dandiliker et al., 1997; Fermeglia et al., 2001), surface-coating dendritic sensors (Valerio et al., 1997; Balzani et al, 2000), energy funnels (Jiang and Aida, 1997; Adronov et al, 2000), and building blocks for more elaborate supermolecular structures (Emrick and Frechét,

1999).

The molecular features enabling these applications are persistent and controllable nanoscale dimensions in the range from 1 to 100 nm, some control over shape via molecular design of the dendrimer core, precise masses that can approach 100,000 (with practically no polydispersity, i.e. $M_w/M_n \approx 1$), chemicaòòy reactive su5rface functionality, interiors that can be specifically tailored to hydrolytically or thermally demanding environments, and designed solvophilicity at the surfaces (even with controlled, local variation over the surface of the same molecule).

Polyphenylene – compounds containing benzene rings linked by σ-bonds – form an increasingly important class of organic materials, as the benzene ring is an extremely flexible modulus for the construction of a wide range of structures and can bear a large range of active functionality (Grimsdale and Müllen, 2001). Also, the delocalized π-systems on adjacent rings can overlap to form extended conjugate assemblies, which can be of considerable importance in material science, as their optical and electrical properties make them suitable for use as active compounds in a variety of electronic devices, including light-emitting diodes (LEDs) (Kraft et al., 1998), optically-pumped lasers (Tessler, 1999), and field-effect transistors (FETs) (Horowitz, 1998).

Tetrahedral polyphenylene dendrimers (PD), alias cascade molecules with four successively branched arms made of phenyl rings only and emanating from a central core, are a new class of dendritic materials that have been recently synthesized by Müllen and coworkers (Morgenroth and Müllen, 1997; Berresheim et al., 1999). In particular, they introduced 3,4-bis(4-triisopopylsilylethynyl-phenyl)-2,5-diphenylcyclopenta-2,4-dienone (**1a**) as a building block for the synthesis of a new type of nanosized hydrocarbon dendrimers. The key-step of their dendrimer synthesis

is the [2+4]cycloaddition of **1a** to a core, such as 3,3',5,5'-tetraethynylbiphenyl (**1b**) or tetra-(4-ethynylphenyl)methane (**1c**) (Scheme 1).

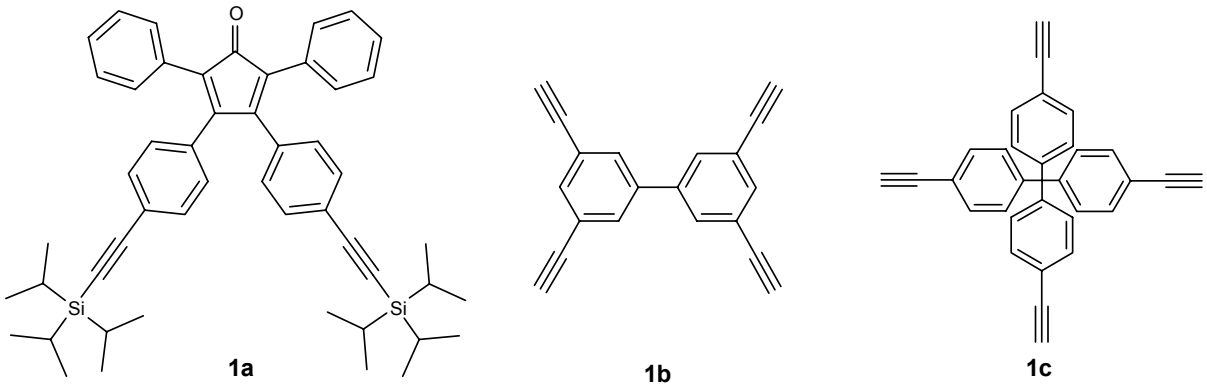

Scheme 1. Building block and two tetrafunctionalized cores leading to PDs.

After cleavage of the triisopropylsilyl groups, the obtained oligoethynyl is ready for further Diels-Alder reactions. Thus, by this repetitive cycloaddition-deprotection sequence, the construction of dendrimer generations G1 (**2b** and **2c**), G2 (**3b** and **3c**) and G3 (**4b** and **4c**) can be accomplished (see Scheme 2).

The surface of theses dendrimers can be coated with a wide variety of functionalities, including halo, cyano, carboxy, amino, hydroxyl e thiomethyl groups (Wiesler et al., 2001). The amine and carboxy substituents especially should not only provide a means for obtaining water solubility but also for attaching a wide range of other groups to the dendritic nanoparticles, e.g. peptides, antigens or other biological substrates.

Due to their very dense intramolecular packing, these monodisperse polyaromatic dendrimers are of particular interest with respect to the design of nanostructures characterized by an invariant shape (Percec et al., 1998). Besides their significantly enhanced thermal and chemical stability, their postulated rigidity as compared to aliphatic dendrimer systems, coupled with the wide variety of possible

functionalizations, provide the basis for their potential applications, such as support for catalysts, dyes or biological/biomedical active substances in human diagnosis and medicine. All this application potentials, however, will not be realized before the understating of their physical properties is considerably advanced.

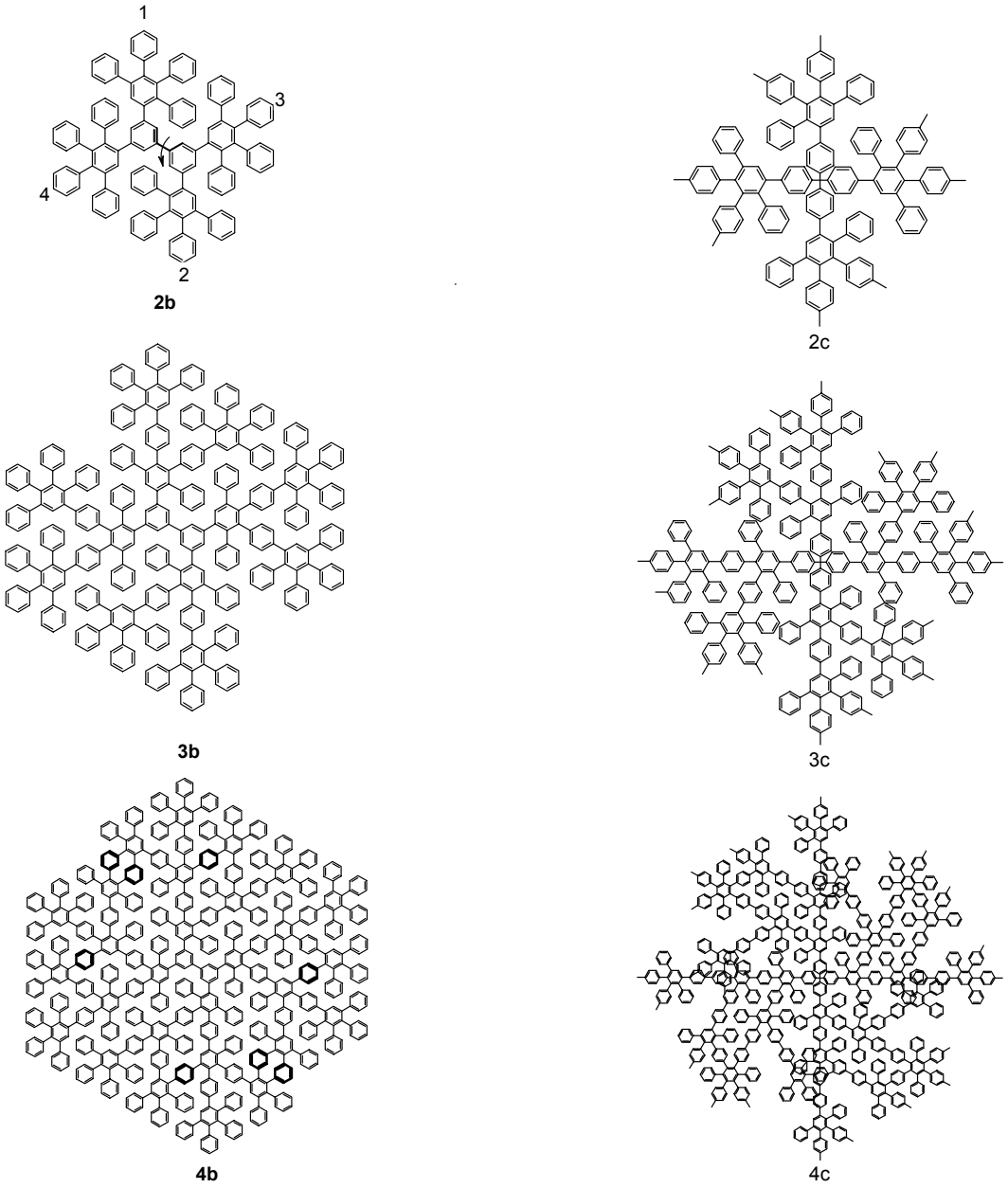

Scheme 2. Nanosize PDs synthesized from cores 1b and 1c.

Notwithstanding the fact that both scattering and microscopic methods have

successfully been applied to the structural characterization of polyaromatic dendrimers (Zhang et al, 2000), attempts to understand their dynamic behavior have been confined to limited, preliminary molecular dynamics simulations (Morgenroth et al., 1997; Brocorens et al., 1999; Wind et al, 2001). Since the knowledge of the global shape and extent of flexibility are among the most important criteria for the design of well defined architectures, in this work we have performed an investigation of the dynamics of amorphous bulk dendrimers based on cores **1b** and **1c** and up to generation 3 by means of accurate molecular dynamics simulations.

2. COMPUTATIONAL DETAILS

All molecular mechanics and dynamics simulations were performed by using the program packages Cerius[2], Discover, Materials Studio (all from Accelrys Inc., San Diego, USA) and in-house developed codes (stand-alone and add-on to the commercial software).

An *ad hoc*, *ab initio* all-atom force field (FF), recently developed by Fermeglia et al. (2003) for PDs was employed in all calculations. Since a detailed description involved oin each step of the development of the FF for PDs is reported in the relevant paper (Fermeglia et al. 2003), only the main features of the force field are briefly outlined below. The bond terms of the FF potential energy function include a simple harmonic function both for bond stretching and angle bending, and a three-terms Fourier expansion for torsions. Finally, a 9-6 Lennard-Jones function is used to represent the van der Waals forces, while the electrostatic interaction is written in the form of a standard Coulomb interaction with partial atomic charges:

The generation of accurate PD model structures was conducted as follows. For each dendrimer generation, the molecule was built and its geometry optimized via a

combined steepest descent – conjugate gradient algorithm, using as a convergence criterion for the energy gradient the root-mean-square of the Cartesian elements of the gradient equal to 10^{-4} kcal/(mol Å). Long-range nonbonded interactions were treated by applying suitable cutoff distances, and to avoid the discontinuities caused by direct cutoffs, the cubic spline switching method was used. Van der Waals distances and energy parameters for nonbonded interactions between heteronuclear atoms were obtained by the 6^{th}-power combination rule proposed by Waldman and Hagler (1993). Such a straightforward molecular mechanics scheme was likely to trap the simulated system in a metastable local high-energy minimum. To prevent the system from such entrapments, the relaxed structures were subjected to a combined molecular mechanics/molecular dynamics simulated annealing (MDSA) protocol (Fermeglia and Pricl, 1999). Accordingly, the relaxed structures were subjected to 5 repeated temperature cycles (from 298 K to 1000 K and back) using constant volume/constant temperature (NVT) MD conditions. At the end of each annealing cycle, the structures were again energy minimized to converge below 10^{-4} kcal/(mol Å), and only the structures corresponding to the minimum energy were used for further modeling.

The calculation of molecular surfaces was performed using the so-called Connolly dot surfaces algorithm (Connolly, 1983 and 1985). Accordingly, a probe sphere of given radius p_r, representing the solvent molecule, is placed tangent to the atoms of the molecule at thousands different position. For each position in which the probe does not experience van der Waals overlap with the atoms of the molecule, points lying on the inward-facing surface of the probe sphere become part of the molecule *solvent-accessible surface* (S_{AS}). According to this procedure, the molecular surface generated consists of the van der Waals surface of the atoms which can be touched by a solvent-sized probe sphere (thus called *contact surface*), connected by a network of concave

and saddle surfaces (globally called *reentrant surface*), that smoothes over crevices and pits between the atoms of the molecule. The sum of the contact and the reentrant surface forms the so-called *molecular surface* (MS); this surface is the boundary of the *molecular volume* (MV) that the solvent probe is excluded from if it is not to undergo overlaps with the molecule atoms, which therefore is also called *solvent-excluded volume*. Finally, performing the same procedure by setting the probe sphere radius equal to zero, the algorithm yields the *van der Waals surface* (WS).

The details of the isolated dendrimer structures at 298 K were obtained by performing MD simulations under isocoric/isothermal (NVT) conditions. Each molecular dynamics run was started by assigning initial velocity for atoms according to Boltzmann distribution at 2 x T. Temperature was controlled via weak coupling to a temperature bath (Berendsen et al., 1984), with coupling constant τ_T=0.01 ps. The Newton molecular equations of motion were solved by the Verlet leapfrog algorithm using an integration step of 1 fs and for a total simulation time of 3 ns.

3. RESULTS AND DISCUSSION

Figures 1 and 2 show the molecular models of generation 1, 2 and 3 for the **1-b**-based and the **1c**-based dendrimers, respectively, obtained as a result of the first structural investigations performed with MD simulations under NVT conditions. An accurate analysis of the molecular trajectories reveals that, in spite of intramolecular dynamics involving rearrangements of the dendritic arms, as well as of the pentaphenyl benzene units, the global shape of both dendrimeric series does not change throughout the simulation, and the systems retain their overall nano-architecture.

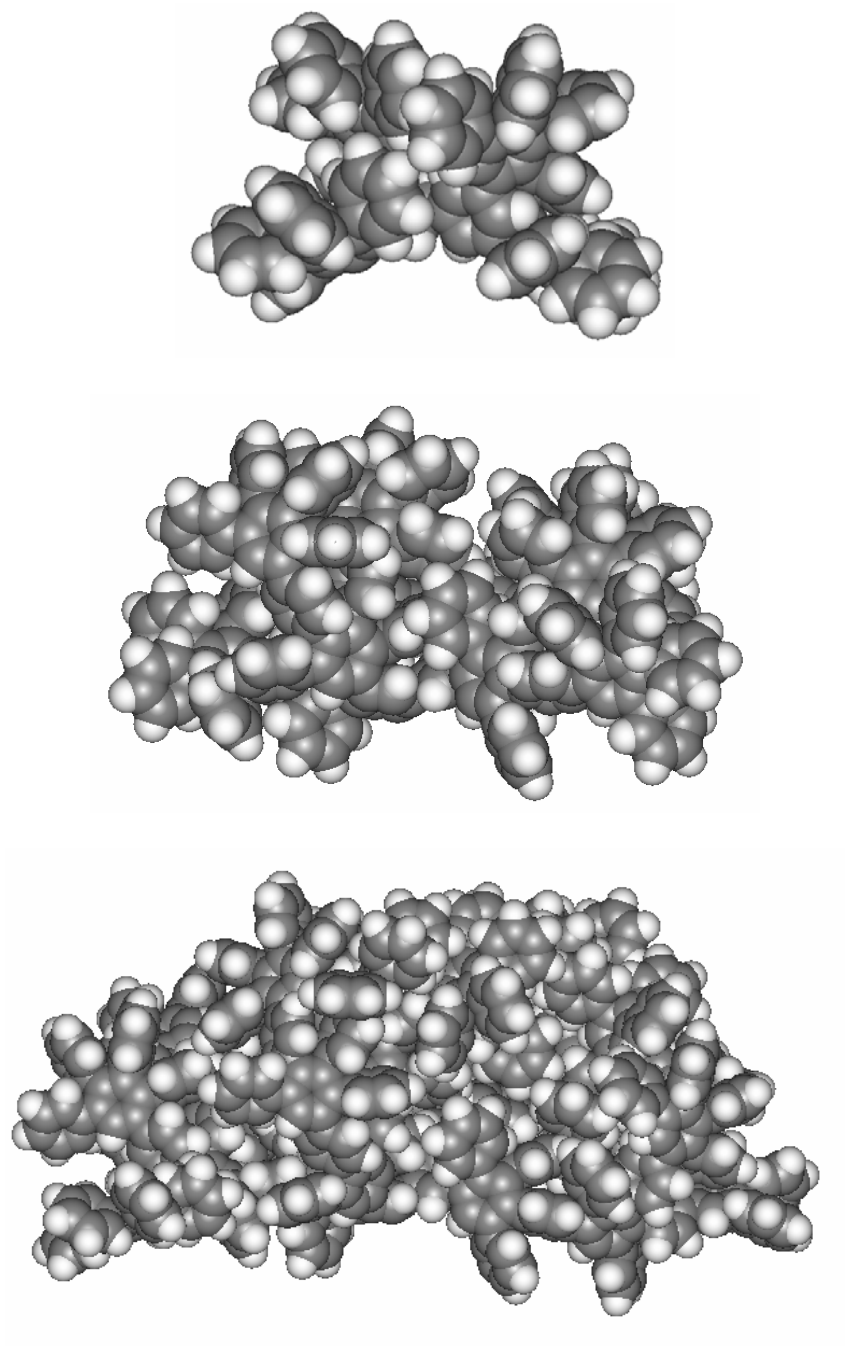

Figure 1. Optimized molecular models of G1 (top), G2 (middle) and G3 (bottom) of PD with core **1b**.

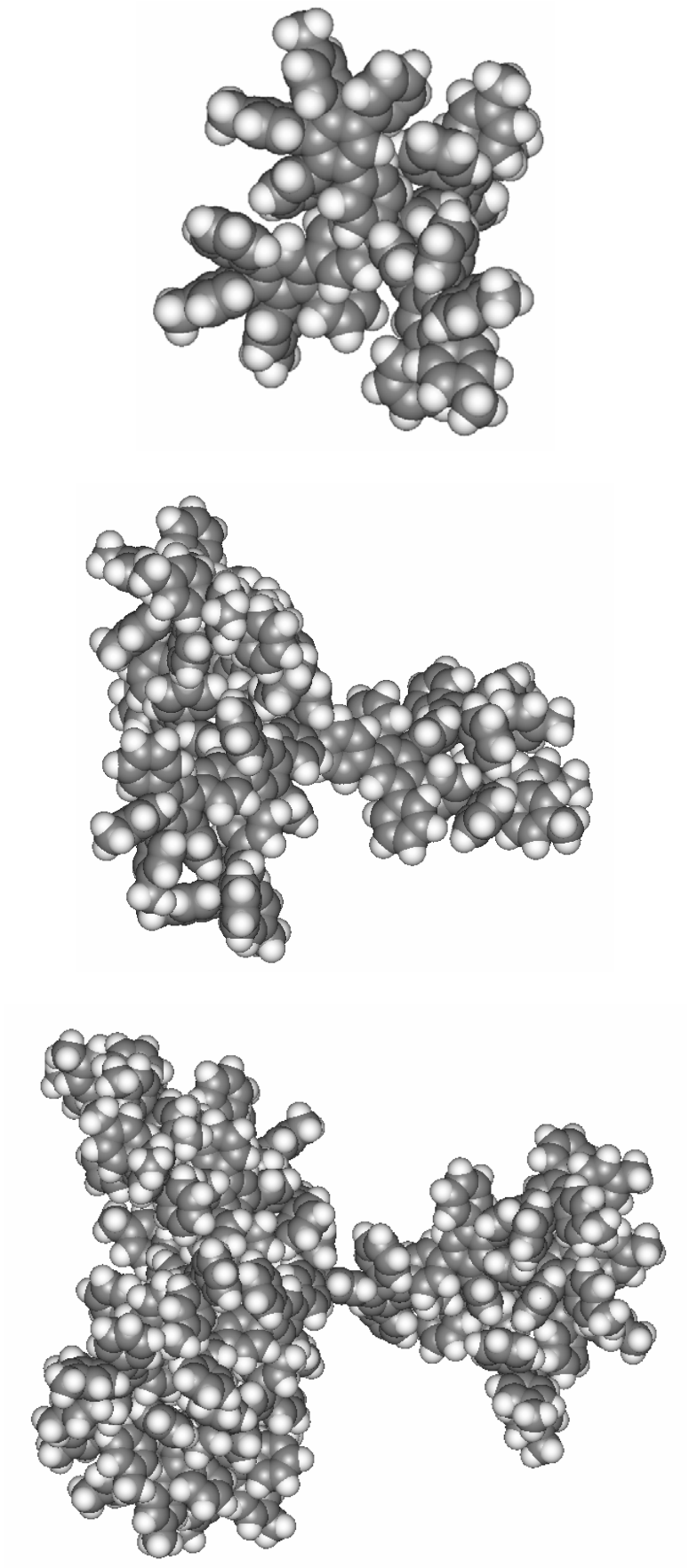

Figure 2. Optimized molecular models of G1 (top), G2 (middle) and G3 (bottom) of PD with core **1c**.

As we may see in Figure 1, the **1-b** based dendrimers grow in a fan-like shape. Indeed, all three generations preserve a flat, central zone around which the structure develops in a somewhat regular fashion. This structural feature is expected to affect the dynamics of the molecule; this can be followed by the evolution of the torsion angles θ_1, which define the relative orientation of the benzene rings of the central core (see the labeling in Scheme 2, upper left). Such analysis reveals that, for higher dendrimer generations and during the entire runs of the dynamic simulations, the peculiar fan-like structure is preserved, and the major movements interest the outer groups. In fact, for the first generation G1-**1b**, the torsion angle value θ_1 varies with amplitude of 13º around its average value of 59º. Accordingly, the distances 1-2 and 3-4 that govern the overall shape of the molecule are only slightly affected by such torsions, being typically of the order of 22 Å and varying by 1 to 5% (0.3 to 1.1 Å) during the entire course of the simulation. In passing to G2-**1b** and G3-**1b**, from a relatively open and symmetrical structure (see Figure 1, top) the dendrimer progressively evolves towards a more compact, skewed structure, characterized by a flat, central zone resembling a Spanish fan (see Figure 1, center and bottom). The evolution of the structure is intimately related to the dynamics of the core and of the G1-**1b** tetraphenylbenzene units. In fact, although the dynamics reveal a tendency of the two units to get closer due to mutual attractive interactions, a strong coupling between the G2-**1b** units of these two branches cannot take place due to the steric constraints in the G1-**1b** layer that limit the molecular mobility. The modification of the form is actually driven by a change in the torsion angle θ_1, which decreases to an average value of 37º (± 7º). Correspondingly, stabilizing van der Waals and Coulomb interactions then lead to the bending and association of the branches. As a results, distance 1-2 increases to ~ 38 Å while distance 3-4 lengthens to approximately 29 Å.

An utterly analogous situation is encountered in the next generation G3-**1b**, where the molecule is characterized by almost the same average value of the torsion angle θ_1 (38º ± 10º) and again two different values of the distances 1-2 (48 Å) and 3-4 (38 Å), respectively.

For the dendrimer with a tetrahedral core **1c**, if the most stable conformation of the first generation is also characterized by an almost symmetrical shape, with an average value of the angle at the central, tetrahedral carbon of 109º (± 3º) (see Figure 2, top), upon growing generation the formation of pairs of tetraphenylbenzene units takes place. Indeed, passing from G1-**1c** to G2-**1c** and G3-**1c**, the pairing of the branches has important consequences on the morphology of the molecule since a) it leads to the formation of an asymmetric diabolo-like molecular shape, formed by a concave part having a high packing density of phenylene rings (see Figure 2, center and bottom), and b) we observe an asymmetric growing of the molecular structure, characterized by a larger increase in the length with respect to the width of the dendrimer (see below). These corresponds to a bimodal distribution of the angle values around the core carbon atom centered, for G2-**1c**, around the average values of 103º (± 3º) and 113º (± 3º), and for G3-**1c** around 101º (± 3º) and 114º (± 3º), respectively The asymmetry in higher generation structures gives rise to different mobility of the branches, which are essentially governed by steric constraints imposed by the relative orientations of the two branches in a given pair. The MD simulations show that this dendrimer family has good shape persistence; despite the fact that the global shape of the dendrimer does not evolve throughout the simulation, local rearrangements of the G2 and G3 tetrephenylbenzene groups can take place in the arms, leading to exchange in the inner vs. outer positions of the peripheral units.

This pictorial evidence can be quantified by the aspect ratio of principal moments of

inertia for various generations G of both PD series (see Figure 3). In the case of the **1b**-based nanoparticles, the main aspect ratio (I_x/I_z) remains constant and approximately equal to 2 with increasing G, since the planar, rigid biphenylenic nucleus does not undergo considerable distortions as the number of lateral ramifications increases. Similarly, the I_z/I_y and the I_y/I_x ratios only very slightly increase and decrease with respect to an average values of 0.76 and 0.63, respectively. In the case of the alternative series, the behavior is somewhat similar, although two ratios, i.e. I_x/I_z and I_z/I_y, are almost coincident and slightly increase from 1 to 1.4, with an average value of 1.2, whereas the third ratio I_y/I_x is practically constant to 0.67.

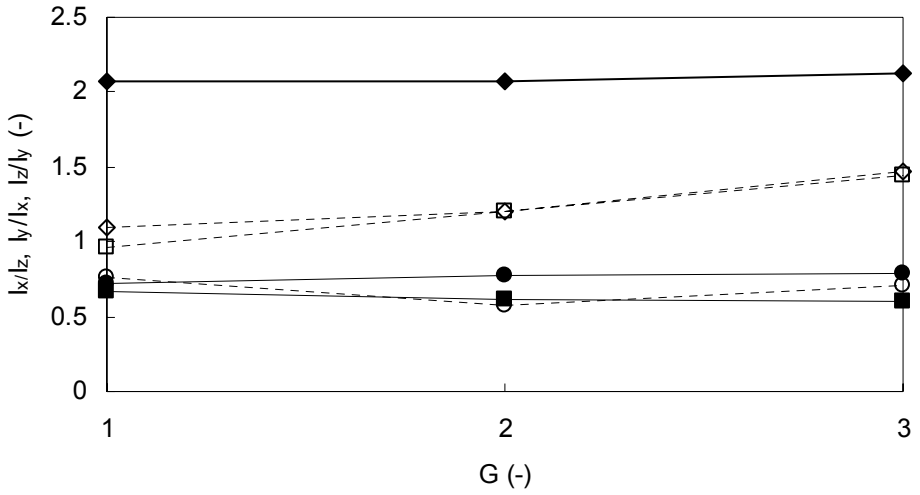

Figure 3. Aspect ratios for both PDs series. Filled symbols: PD-**1b**; open symbols: PD-**1c**. Diamonds: $I_x/_z$; circles: I_y/I_x; squares; I_z/I_y. Lines serve as guide for the eye.

For both dendrimeric series, the overall molecular dimensions deduced from the MD trajectories are reported in Table 1:

Table 1. Overall molecular dimensions (Å) of the first three generations of PDs based on cores **1b** and **1c**.

	G1	G2	G3
PD-**1b**	23 ± 0.3	35 ± 0.5	53 ± 0.7
PD-**1c**	26 ± 0.2	39 ± 0.5	55 ± 0.7

Such data are in excellent agreement with the corresponding, experimental observations by atomic force microscopy, transmission electron microscopy and light scattering measurements (Grimsdale and Müllen, 2001; Kraft et al., 1998).

The radius of gyration R_g is a fundamental tool for the characterization of the structural properties of dendrimers. This quantity is defined as the square root of the second invariant of the first order tensor **S**, which accounts for the spatial distribution of the atom chains by mediating over all N molecular components. The R_g values estimated by molecular dynamics simulations for all generations of both series of PD molecules are plotted in Figure 4 as a function of the dendrimer molecular weight M_w.

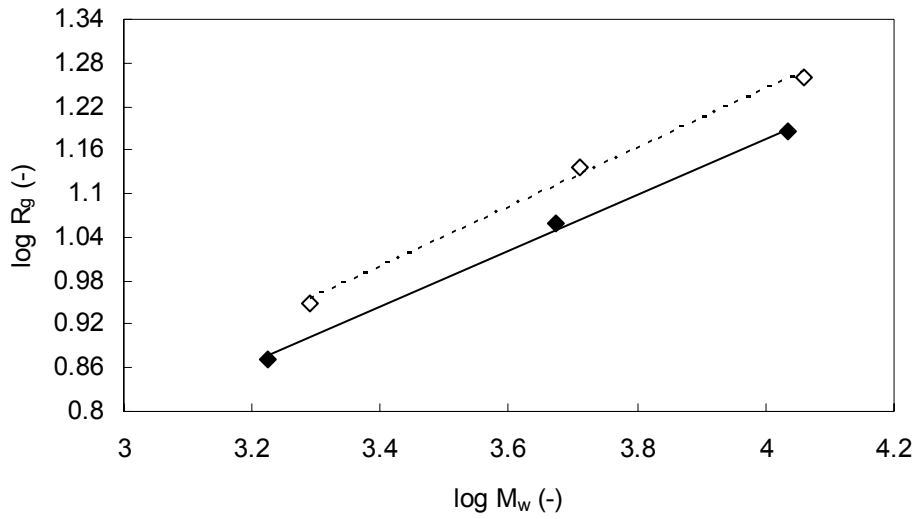

Figure 4. Relationship between radius of gyration R_g and molecular weight M_w for both PD series. Filled diamonds: PD-**1b**; open diamonds: PD-**1c**. Symbols: calculated values; lines: best-fit.

The linear relation between log R_g and log M_w is a further indication for a compact space filling structures with fractal dimensionality d_f of about 2.6 in the case of **1b**-PDs, and 2.5 in the case of **1c**-based dendrimers, respectively.

Fractal geometry is a mathematical tool for dealing with complex systems that have no characteristic length scales. Scale-invariant systems are usually characterized by non-integer (i.e., fractal) dimensions, and hence the objective of any fractal analysis is

to find a relationship of some kind of power-law:

$$\text{physical property} \propto \text{variable}^{\text{scaling exponent}} \quad (1)$$

where the variable and the exponent are related to the fractal dimension. This relation is obviously one that can cover a very broad range of molecular structures; however, this kind of power law requires some symmetry in these structures. Interestingly enough, the values of d_f calculated for both PD series considered are close to the average mass fractal dimension exhibited by the vast majority of proteins (Birdi, 1993), i.e. 2.6-2.7, and to the exponent characterizing the distribution of masses of an ideally branched polymer (d_f = 2.5). Arteries and veins in mammalian vascular systems, too, have been found to obey the scaling law (1) over a range of 20 bifurcations between heart and capillaries. Estimates of the relevant scaling exponent (Tsuchida et al., 1993) give values again near 2.7. Another interesting example is the branching pattern of arterial kidney vessels, which is characterized by fractal geometry with fractal dimensions between 2.0 and 2.5 (Sernetz et al, 1992). This is a reasonable value for biological evolution to have attained, given the requirement that arteries and veins should come close to every point of the body that needs nourishment and waste disposal. But the ideal value of d_f = 3 for this purpose is, of course, unattainable, because a space-filling vascular system leaves too little tissue for other tasks.

One of the important problems in supramolecular chemistry is the origin of specificity and recognition in molecular interactions. An essential step in this process is complementary contact between approaching molecular surfaces. Surface representations of macromolecules such as, in our specific case, proteins or dendrimers, have provided a powerful approach for characterizing the structure, folding, interactions and properties of such molecules. A fundamental feature of

surfaces that has not been characterized by these representations, however, is the texture (or roughness) of polymer surfaces, and its role in molecular interactions has not been defined. Another important, related issue deals with a basic property of surface fractals: their accessibility to incoming molecules depends on their size. We analyze here the implications of these properties on the derivatization of PD dendrimer surfaces. Derivatization of surface is a key process, given the ability to fine-tune the type of surface-adsorbate interaction by a suitable choice of the derivatizing agents. Generally, there are three main factors that determine the accessibility of derivatizable spots to reaction. The first is the umbrella effect of the reagent, as most reagents have cross-sectional areas that shield more than the molecular locus with which they react. The second factor is the surface irregularity, tortuosity, and connectivity, and the degree to which these surface features shield the reactive points from an incoming reagent molecule. The third parameter is surface heterogeneity, from the point of view of both the possible clustering of reactive sites and the difference in reactivities of the terminal groups due to inductive effects of the surrounding moieties.

It has been long known in surface science that apparent surface areas decrease with increase in adsorbate size, due to the parallel decrease in geometric accessibility. It was found that, in many instances, the relation between these two parameters is:

$$m \propto \sigma^{-D/2} \qquad (2)$$

where m is the monolayer value of a physisorbed molecule of cross-sectional area σ, and D is usually interpreted as the fractal dimension of the surface available to adsorption. Since it is found that, usually, $2 \leq D < 3$, it seem that the simplest interpretation of D is that it reflects mainly the geometrical nature of the surface, i.e. from a flat surface ($D = 2$) up to extreme volume-like irregularity ($D = 3$). Equation

(2) may be applied, in principle, for the evaluation of the surface roughness and surface accessibility of macromolecules, such as proteins and dendrimers. The degree of geometric irregularity of a dendrimer is one of the parameters which determine the diffusion kinetics of a small substrate on the surface of the macromolecule or into it. The method of determining the *D* value of dendrimers (Blasizza et al., 2000; Fermeglia et al., 2002) has been to apply Eq. (2) by "covering" the surface of the PDs with a monolayer of model spherical molecules of cross-sectional area σ. The area *A* thus determined is:

$$A \propto \sigma^{(2-D)/2} \tag{3}$$

Such a relationship is illustrated in Figure 5 for the three generations of the **1b**-based series of dendrimers, as an example.

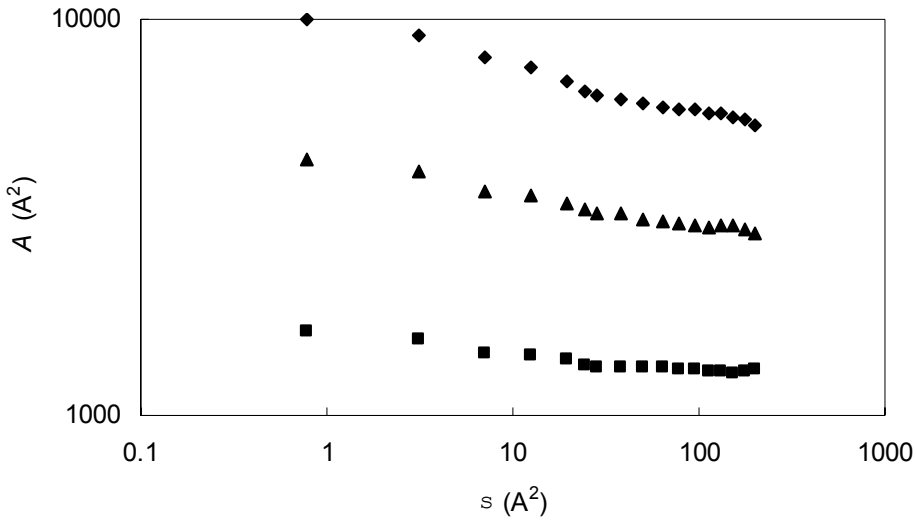

Figure 5. Double logarithmic plot of the molecular surface area *A* as a function of the probe cross-sectional area σ. for the PD-**1b** series. Diamonds: *G*3-**1b**; triangles: *G*2-**1b**; squares: *G*1-**1b**.

As we may infer from this graph, the slopes of the plots show a tendency to reach a plateau (corresponding to $D = 2$) in the limit of both small and large probe sizes. Small probes predominantly interact with the smooth van der Waals spheres describing the dendrimer atoms, whereas large probes are sensitive to the overall

shape of the molecule. For probes in the intermediate range (i.e., 1 – 4 Å), however, the value of *D* increases from 2.06 of G1-**1b** to 2.20 of G3-**1b**. Table 3 tabulates the calculated surface fractal dimensions for both dendrimer series.

Table 3. Surface fractal dimension *D* of the first three generations of PDs based on cores **1b** and **1c**.

	G1	G2	G3
PD-**1b**	2.06	2.14	2.20
PD-**1c**	2.01	2.02	2.04

It is worthwhile noticing that the calculated fractal dimensions for both dendrimer families are quite close to those characterizing various protein and biomacromolecules, which vary, just to cite a few, between 2.05 for DNA to 2.18 of retinol binding protein (Birdi, 1993).

The results of this analysis are of much value, especially in molecular design of pharmaceutical and/or biocompatible molecules, as well as in surface molecular recognition based on similar fractal dimensions. In particular, the surface pattern of both paraphenylene dendrimer series seem to be flatter and regular, being the relevant fractal dimension practically constant and almost equal to 2 with increasing generations. This suggests that, in principle, both these starburst molecules should be easily derivatized, with a few errors and defects even at generation 3.

Other molecular issues deriving from the collected data are the values of van der Waals surface areas (A_{vdW}) and volumes (V_{vdW}), and the so-called molecular solvent accessible surfaces (SAS). The estimated values for the two PDs series are reported in Table 4. In the case of SAS, the relevant values refer to the molecular surface available to water as the solvent, represented as an equivalent probe sphere of radius 1.4 Å (see §2).

Table 4. van der Waals surface areas (A_{vdW}) (Å^2), volumes (V_{vdW}) (Å^3) and molecular solvent accessible surfaces (SAS) (Å^2) for the first three generations of PDs based on cores **1b** and **1c**.

PD-**1b**	G1	G2	G3
A_{vdW}	1748	4860	11067
V_{vdW}	1584	4444	10165
SAS	1340	3310	6600
PD-**1c**			
A_{vdW}	2104	5388	11964
V_{vdW}	1878	4869	10861
SAS	1751	4027	8313

Using the molecular weight and the van der Waals volumes reported in Table 4, we could estimate an approximate value for the density of each dendrimeric structure. This approach allows the comparison of the density between different generations of dendrimers. The calculated values for the two dendrimeric series reveal that, in both cases, the density does not change with in passing from G1 to G3, being equal to 2.0 and 1.7 for the **1b**-based and the **1c**-based molecules, respectively. Keeping in mind that, in this preliminary investigation, solvent effects have been neglected, these results reflect only the effect of molecular structure variations upon density emphasizing the relative differences between different generations. That is, the data clearly show that there is no change in density with increase generation number, in accordance with the shape-persistence of both dendrimer series.

As mentioned earlier, parameters such as size, shape and multiplicity are transcribed, and displayed throughout the dendrimer development. These variables can have dramatic effects on the ultimate shape, the interior topology and the exterior surface properties (alias congestion) of the developing dendrimer.

Mathematically, we can appraise dendrimer surface congestion as a function of generation from the following relationship:

$$A_Z = \frac{A}{N_Z} \propto \frac{R^2}{N_c N_b^G} \tag{4}$$

in which A_Z is the surface area per terminal group Z, A is the dendrimer surface area and N_Z is the number of terminal groups Z per generation (Tomalia et al, 1990).

From this relation we can see that, at higher generations G, the surface area per Z group should become increasingly smaller and experimentally approach the cross sectional area of the van der Waals dimension of the surface group Z. The generation G thus reached is referred to as the *starburst dense-packed (limited) generation*. As predicted by de Gennes and Hervet (1983), ideal starburst growth without branch defects is possible only for those generations preceding the dense-packed state. This critical dendrimer property gives rise to self-limiting starburst dimensions, which are a function of the branch-segment length *l*, the core multiplicity N_c, the branch-juncture multiplicity N_b and the sterical dimensions of the terminal group Z. Since the dendrimer radius R in the expression above is dependent of *l*, larger *l* values will delay this congestion, whereas larger N_c and N_b values and larger Z dimensions will dramatically hasten it.

Computer-assisted molecular simulations allowed us to determine the surface area per Z group, A_Z, as a function of generation for both PDs series (see Figure 6). For both dendrimer families, A_Z increases from generation 1 to 3, but the rate of increase progressively diminishes, owing to the beginning of surface congestion. Quite a similar behavior seems to characterize other starburst molecules of different nature (Tomalia et al., 1990; Blasizza et al, 2000; Gelmetti et al., 2001; Fermeglia et al., 2002). Accordingly, this analysis allows us to conclude that, for this type of dendrimers, the starburst limited generation, that is the generation at which the molecule should exhibit (1) sterically inhibited reaction rates, (2) sterically induced

stoichiometry, and, quite possibly, (3) a critical phase change due to surface cooperativity is presumably located in correspondence of G3. Such a conclusion has been theoretically anticipated by Grimsdale and Müllen (2001), and this study seems to confirm their hypothesis.

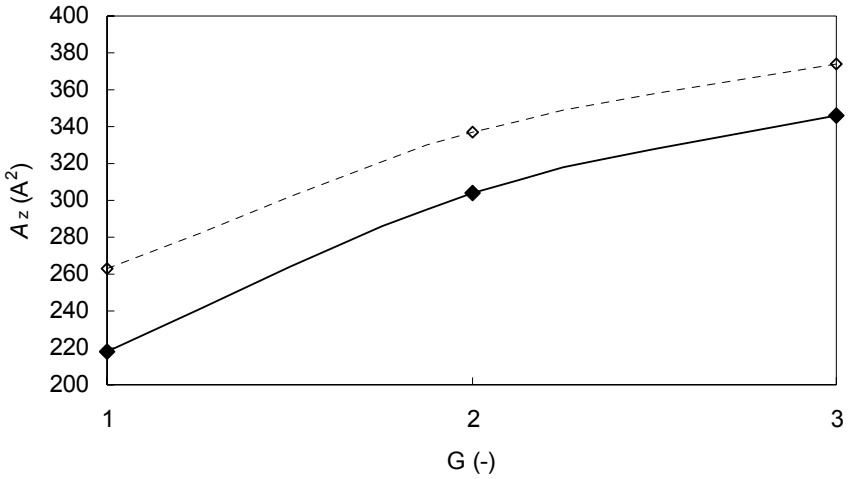

Figure 6. Surface area per terminal group vs. generation for the two PD series. Filled diamonds: PD-**1b**; open diamonds: PD-**1c**. Symbols: calculated values; lines serve as guide for the eye.

Finally, we report in Table 5 the calculated values of the dipole moment of each dendrimer series generations.

Table 5. Dipole moment μ (Debye) of the first three generations of PDs based on cores **1b** and **1c**.

	G1	G2	G3
PD-**1b**	1.5	2.5	3.8
PD-**1c**	1.1	2.7	3.4

As we may see, the two series are characterized by similar, low values of this quantity. Although no μ data are available in literature for these substances, the MD simulated values of the dipole moments for the corresponding nuclei (0.3 D for **1b**

and 0.4 D for **1c**) and the fact that PDs are based solely on aromatic repetitive units can account for the values reported in Table 5.

4. CONCLUSIONS

3D polyphenylene dendrimers (PDs) can be prepared in ways that enable control of their shape, and their surfaces can be selectively functionalized in ways that enable them to be used as functional nanoparticles with a wide variety of possible applications. For instance, amine and hydroxyl groups especially could not only provide a means for obtaining water solubility through attachment of, for instance, polyethylene oxide or peptide chains, but also for attaching a further variety of groups to the dendritic nanoparticles. As the full range of possible exploitations of PDs has just begun to be explored, and can we cannot predict what will be discovered once one ventures out into this vast area of unexplored territory, we employed accurate, atomistic molecular dynamics simulations (MD) to probe the shape and internal organization of two PD families based on two different cores. Particular care was taken to ensure complete structural equilibration by using an ad hoc developed force field and implementing a MD simulated annealing protocol prior to evaluation of the molecular structure and dynamics. Both dendrimer families were found to be characterized by molecular dimensions in the nano-range, and by a shape-persistent, non-spherical structure, of molecular fractal dimension around 2.5-2.6, and of surface fractal dimension practically constant and almost equal to 2 with increasing generations in both cases. The MD analysis revealed also that, for this type of dendrimers, the starburst limited generation, i.e. the generation number at which brach defect and surface congestion phenomena begin to appear, is presumably located in correspondence of the third generation.

5. REFERENCES

Adronov, A., Gilat, S.L., Frechét, J.M.M., Ohta, K., Neuwahl, F.R.V., Fleming, G.R., *J. Am. Chem. Soc*. 122 (2000) 1175.

Balzani, V., Ceroni, P., Gestermann, S., Kauffmann, C., Gorka, M., Vögtle, F., Chem. Commun. (2000) 853.

Berendsen, H.J.C. Postma, J.P.M. van Gunsteren, W.F. DiNola, A. Haak, J.R. *J. Comput. Phys*. 81 (1984) 3684.

Berresheim, A.J., Müller, M., Müllen, K., *Chem Rev*. 99 (1999) 1747.

Birdi, K.S., *Fractals in Chemistry, Geochemistry and Biophysics*, Plenum Publishing Corporation: New York (1993).

Blasizza, E., Fermeglia, M., Pricl, S., *Molecular Simul*. 24 (2000) 167.

Brocorens, P., Zojer, E., Cornil, J., Shuai, Z., Leising, G., Müllen, K., Brédas, J.L., *Synth. Met*. 100 (1999) 141.

Brunner, H., *J. Organomet. Chem*. 500 (1995) 39.

Connolly, M.L. *Science* 211 (1983) 709.

Connolly, M.L. *J. Am. Chem. Soc*. 107 (1985) 1118.

Dandiliker, P.J., Diederich, F., Zingg, A., Gisselbrecth, J.P., Gross, M., Louati, A., Sanford, E., *Helv. Chim. Acta* 80 (1997) 1773.

de Gennes, P.G., Hervet, H.J., *Phys. Lett*. 44 (1983) 351.

Dykes, G.M., *J. Chem. Technol. Biochem*. 76 (2001) 903.

Emrick, T., Frechét, J.M.J., Curr. Opin. Coll. Interface Sci. 4 (1999) 15.

Esfand, R., Tomalia, D.A., *Drug Discovery Today* 6 (2001) 427.

Fan, Q.H., Chen, Y.M., Chen, X.M., Jiang, D.Z., Xi, F., Chan, A.S.C., *Chem. Commun*. (2000) 789.

Fermeglia, M., Ferrone, M, Pricl, S., *Bioorg. Med. Chem*. 10 (2002) 2471.

Fermeglia, M., Ferrone, M, Pricl, S., *J. Phys. Chem. A* in press (2003).

Fermeglia, M., Pricl, S. *AIChE Journal* 45 (1999) 2619.

Fischer, M., Vögtle, F. *Angew. Chem. Int. Ed. Engl.* 38 (1999) 884.

Frechét, J.M.J., *Science* 263 (1994) 1710.

Gelmetti, S., Fermeglia, M., Pricl, S., *Proceedings of the AIChE Annual Meeting on CDROM,* Reno, NV, USA, Nov 4-9 (2001).

Grimsdale, A.C., Müllen, K., *The Chemical Record* 1 (2001) 243.

Hawker, C.J., Wooley, K.L., Frechét, J.M.J., *J. Chem. Soc. - Perkin Trans. 1* (1993) 1287.

Horowitz, G., *Adv. Mater*. 10 (1998), 365.

Kraft, A., Grimsdale, A.C., Holmes, A.B., *Angew. Chem. Int. Ed.* 37 (1998) 402.

Jiang, D.L., Aida, T., *Nature* 388 (1997) 454.

Lynn, D.M., Langer, R., *J. Am. Chem. Soc*. 122 (2000) 10761.

Mekelburger, H.-B., Jaworek, W., Vögtle, F., *Angew. Chem. Int. Ed. Engl.* 31 (1992) 1571.

Morgenroth, F., Müllen, K., *Tetrahedron* 53 (1997) 15349.

Morgenroth, F., Kübel, C., Müllen, K., *J. Mater. Chem*. 7 (1997) 1207.

Ohashi, S., Kubo, T., Ikeda, T., Arai, Y., Takahashi, K., Hirasawa, Y., Takigawa, M., Satoh, E., Imanishi, J., Mazda,n O., *J. Orthop. Sci*. 6 (2001) 75.

Pan, Y.J., Ford, W.T., *Macromolecules* 33 (2000) 3731.

Percec, V., Ahn, C.-H., Ungar, G., Yeardley, D.J.P., Möller, M., Sheiko, S.S., *Nature* 391 (1998) 161.

Sernetz, M., Wübbeke, W.B., Wlczek, P., *Physica A* 191 (1992) 13.

Stiriba, S.-E., Frey, H., Haag, R., *Angew. Chem. Int. Ed. Engl.* 41 (2002) 1329.

Tessler, N., *Adv. Mater*. 11 (1999) 363.

Tomalia, D.A., Naylor, A.M., Goddard, W.A. III, *Angew. Chem. Int. Ed. Engl.* 29 (1990) 138.

Tsuchida, E., Komatsu, T., Arai, K., Nishide, H., *J. Chem. Soc. Dalton Trans*. (1993) 2465.

Valerio, C., Fillaut, J.L, Ruiz, J., Guittard, J., Blais, J.C. and Astruc, D., *J. Am. Chem. Soc.* 119 (1997) 2588.

Voit, B.I., *Acta Polym*., 46 (1995) 87.

Waldmann, M., Hagler, A. T. *J. Comput. Chem*. 14 (1993) 1077.

Wiesler, U. M., Weil, T., Müllen, K., in *Dendrimers III: Design, Dimension, Function*, Vögtle, F., Ed. Topics in Current Chemistry. Springer-Verlag: Berlin, Vol. 212 (2001) 1.

Wind, M., Wiesler, U.-M., Saalwächter, K., Müllen, K., Spiess, H.W., *Adv. Mater*. 13 (2001) 752.

Zhang, H., Grim, P.C.M., Foubert, P., Vosch, T., Vanoppen, P., Wiesler, U.-M., Berresheim, A.J., Müllen, K., De Schyver, F.C., *Langmuir* 16 (2000) 9009.

Acknowledgments

The authors thank the European Commission for partially supporting the research under Project G5ST CT 2000 50007.